

Brachistochrone Curve Representation via Transition Curve

Rabiatul Adawiah Fadzar*, Md Yushalify Misro

School of Mathematical Sciences, Universiti Sains Malaysia, Malaysia

*Corresponding Author: rabiatul.fadzar@gmail.com, yushalify@usm.my

Received September 21, 2022; Revised October 23, 2022; Accepted November 23, 2022

Cite This Paper in the following Citation Styles

(a): [1] SRabiatul Adawiah Fadzar, Md Yushalify Misro, "Brachistochrone Curve Representation via Transition Curve," *Mathematics and Statistics*, Vol.11, No.1, pp. 213-222, 2023. DOI: 10.13189/ms.2023.110125

(b): Rabiatul Adawiah Fadzar, Md Yushalify Misro, (2023). *Brachistochrone Curve Representation via Transition Curve. Mathematics and Statistics*, 11(1), 213-222. DOI: 10.13189/ms.2023.110125

Copyright ©2023 by authors, all rights reserved. Authors agree that this article remains permanently open access under the terms of the Creative Commons Attribution License 4.0 International License

Abstract The brachistochrone curve is an optimal curve that allows the fastest descent path of an object to slide frictionlessly under the influence of a uniform gravitational field. In this paper, the Brachistochrone curve will be reconstructed using two different basis functions, namely Bézier curve and trigonometric Bézier curve with shape parameters. The Brachistochrone curve between two points will be approximated via a C-shape transition curve. The travel time and curvature will be evaluated and compared for each curve. This research revealed that the trigonometric Bézier curve provides the closest approximation of Brachistochrone curve in terms of travel time estimation, and shape parameters in trigonometric Bézier curve provide better shape adjustability than Bézier curve.

Keywords Brachistochrone Curve, Bézier Curve, Trigonometric Bézier Curve, C-shape Transition Curve, Travel Time, Curvature

1 INTRODUCTION

Brachistochrone curve has the shortest travel time compared to other types of curves. The Brachistochrone problem was solved by Johann Bernoulli using the calculus of variation and Euler-Lagrange [1]. Brachistochrone comes from two Greek words; *Brachistos* which means shortest, while *Chronos* means time [2]. An object will travel frictionlessly along this curve under the influence of gravitational force in the shortest period of time. An object will slide to the end point with the same amount of time on a Brachistochrone curve, regardless of the position of the object. Brachistochrone curves are useful for engineers and drafters in designing roller coasters, since they need to accelerate the car to the highest speed possible and in the quickest possible vertical drop. Brachistochrone curves are also useful in the designing of racetracks, ski jumps, and skate park bowls[1].

Bézier curves and surfaces is widely utilized in computer graphics and engineering. Parametric equation of the Bézier curve is applicable in the calculation of curve's distance, velocity, travel time, and curvature. The curvature has been applied in the estimation of road speed by approximating the actual shape of the road and verifying the result using manual calculation of the curvature on the map [3]. Another researcher used fundamental concept in Bézier curve to compute the design speed by fitting the road's curve continuously [4]. More application of quintic trigonometric Bézier curve is found in [5], where they calculated a maximum speed estimation and discovered that a minor change in coordinates would alter the curvature of the curve. [6] proposed a flexible curve to facilitate the alteration of the curve without changing the control polygon. Recently, Bézier-like or aesthetic Bézier curve have been prominently studied [7, 8, 9]. Some of the aesthetic curves are used to construct spiral and transition curves.

Transition curve is extremely useful in highway and railway designs. Research in [10] was expanded by [11], who proposed a new adaptive algorithm of S-shape and C-shape transition curves by determining the formulas in different parameters for the G^2 transition curves. The generation of S- and C-shaped transition curves with basis functions composed of shape parameters

was done in [12]. Research on finding the appropriate range of shape parameters in constructing an S- and C-shape transition curve was done in [13], and they concluded that shape parameters play an important role in constructing a fair curve. Transition curves are produced using various basis functions, such as quintic trigonometric Bézier and GHT-Bézier curves, which have been reported in [14] and [15] respectively.

Each of the basis functions in [12], [14] and [15] is different but it still preserves the properties of the Bézier curve. However, in [14], the authors used degree five which is a quintic trigonometric Bézier curve with two shape parameters while in [15], the authors used cubic GHT-Bézier curve where the basis functions consist of the trigonometric and exponential functions. In this study, the C-shape transition curve using cubic trigonometric Bézier with two shape parameters as in [12] will be extended to reconstruct the Brachistochrone curve. Owing to its unique characteristic and potential number of applications, this study also will be reconstruct the Brachistochrone curve using conventional Bézier curve. The parametric equation of Brachistochrone curve from both curve are able to simplify the computational process, thus, the travel time and curvature will be evaluated and compared for each curve.

2 Mathematical Model

Consider a ball rolling from a starting point at the height of h_0 to the endpoint at the height of h . The force that acts on an object is the gravitational force, g . The sum of kinetic energy, EK and potential energy, PE is constant [16]. The fastest time of an object sliding on the curve depends on the potential energy, kinetic energy, and velocity [1]. Thus, the velocity, v is obtained as follows:

$$mgh_0 = \frac{1}{2}mv^2 + mgh, \quad (1)$$

$$v = \sqrt{2g(h_0 - h)}. \quad (2)$$

with $y_0 = h_0$ and $y = h$. After the starting point, A , and the ending point, B , are fixed, the length between two points, ds , will be obtained using Euclidean distance equation. By having velocity and distance, the travel time, dt will be yield as follows [16]:

$$ds = \sqrt{(dx)^2 + (dy)^2}, \quad (3)$$

$$dt = \frac{ds}{v}, \quad (4)$$

$$T = \int dt. \quad (5)$$

2.1 Calculus Variation and Euler-Lagrange

Calculus variation is used to find the minimum travel time for an object on a curve that falls from $A(x_A, y_A)$ to $B(x_B, y_B)$ under uniform gravitational fields [17] as in Equation (6)

$$T = \int_A^B \frac{ds}{v}, \quad (6)$$

where ds are the arc length of the curve, given as:

$$ds = \sqrt{1 + \left(\frac{dy}{dx}\right)^2} dx. \quad (7)$$

Then, substitute Equation (3) and (7) into Equation (6), we obtained T as follows:

$$T = \int_{x_A}^{x_B} \sqrt{\frac{1 + (y')^2}{2g(h_0 - h)}} dx. \quad (8)$$

To minimize T , let

$$f(x, y, y') = \sqrt{\frac{1 + y'^2}{2g(h_0 - h)}}. \quad (9)$$

As mentioned earlier that $y_0 = h_0$ and $y = h$, calculus variation is required to determine the path $y = y(x)$ between x_A and x_B with a maximum or minimum value of functional L , that is

$$L = \int_{x_A}^{x_B} f(x, y(x), y'(x)) dx. \quad (10)$$

By taking functional L equal to zero as in Equation (11)

$$\delta L = \delta \int_{x_A}^{x_B} f(x, y(x), y'(x)) dx = 0, \tag{11}$$

the extremal condition for L are as follow:

$$\frac{\delta f}{\delta y} - \frac{d}{dx} \left(\frac{\delta f}{\delta y'} \right) = 0. \tag{12}$$

To simplify, there are a few steps are skipped from Equation (11) to Equation (12) and the reader can refer to those steps in [16], Then, by substituting f into Equation (12), the solution is obtained as follows:

$$\sqrt{\frac{1+y'^2}{2g(h_0-h)}} - y' \left(\frac{y'}{\sqrt{2gy(1+y'^2)}} \right) = C. \tag{13}$$

Squaring both sides and rearranging Equation (13) will produced

$$y' = \sqrt{\frac{(2C-y)}{y}}. \tag{14}$$

By integrating Equation (14), the parametric equation of the Brachistochrone curve is formed as follows:

$$x(\theta) = r(\theta - \sin(\theta)) + x_0, \quad y(\theta) = -r(1 - \cos(\theta)) + y_0, \tag{15}$$

where r is the radius of circle that rolls along the straight line, and θ denotes as the angle rotation. Next, Equation (15) will be differentiated and substituted into Equation (8). Then, by integrating Equation (8), the travel time for Brachistochrone curve is calculated as follows:

$$T = \sqrt{\frac{r}{g}} \theta, \tag{16}$$

where g is gravitational value.

2.2 Cubic Bézier Curve

Degree three of conventional Bézier curve using Bernstein polynomial function can be expressed as

$$b(t) = \sum_{i=0}^3 Q_i B_i(t), \quad t \in [0, 1], \tag{17}$$

where Q_i and $B_i(t)$ is a set of points and functions with $i = 0, 1, 2, 3$ respectively. Basis functions of $B_i(t)$ can be defined as:

$$\begin{aligned} B_0(t) &= (1-t)^3, \\ B_1(t) &= 3t(1-t)^2, \\ B_2(t) &= 3t^2(1-t), \\ B_3(t) &= t^3. \end{aligned} \tag{18}$$

2.3 Cubic Trigonometric Bézier Curve

Flexible Bézier-like curve was proposed by [6] are as below:

$$m(t) = \sum_{i=0}^3 P_i n_i(t), \quad t \in [0, 1], \tag{19}$$

where P_i is the control points and $n_i(t)$ is the basis functions that can be denoted as:

$$\begin{aligned} n_0(t) &= \left(1 - \sin \frac{\pi t}{2}\right)^2 \left(1 - \rho \sin \frac{\pi t}{2}\right), \\ n_1(t) &= \sin \frac{\pi t}{2} \left(1 - \sin \frac{\pi t}{2}\right) \left(2 + \rho - \rho \sin \frac{\pi t}{2}\right), \\ n_2(t) &= \cos \frac{\pi t}{2} \left(1 - \cos \frac{\pi t}{2}\right) \left(2 + \sigma - \sigma \cos \frac{\pi t}{2}\right), \\ n_3(t) &= \left(1 - \cos \frac{\pi t}{2}\right)^2 \left(1 - \sigma \cos \frac{\pi t}{2}\right). \end{aligned} \tag{20}$$

Cubic trigonometric Bézier basis functions for two arbitrary real values of $\rho, \sigma \in [-2, 1]$ is depicted in Figure 1.

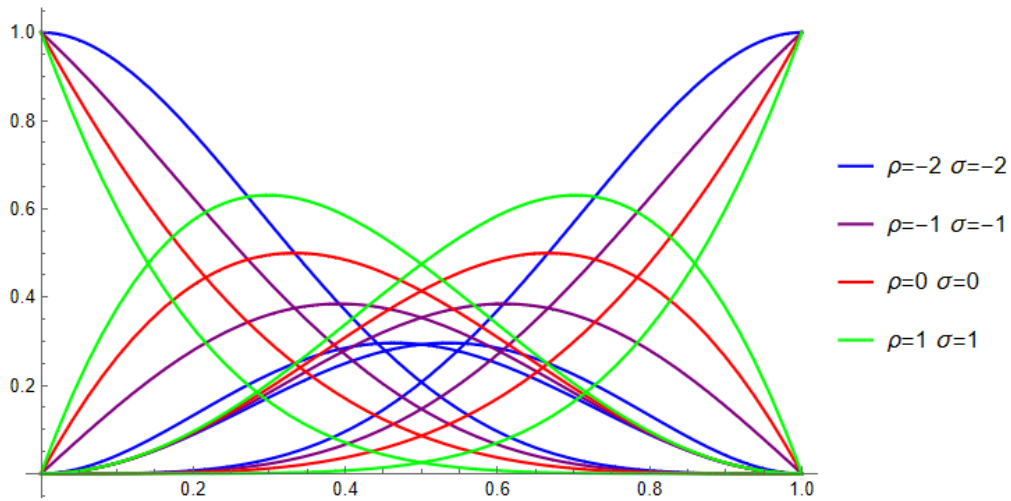


Figure 1. Cubic trigonometric Bézier basis function with shape parameters ρ and σ

2.4 Curvature Computation

In a Cartesian coordinate system, a point a can be defined as a vector $a = (a_x, a_y)$ with the length of vector a is described as follows:

$$\|a\| = \sqrt{(a_x^2 + a_y^2)}. \quad (21)$$

Vector a is said to be parallel to vector b with notation $a \parallel b$. The positive angle of vector a is an angle from the vector $(1, 0)$ to a in anticlockwise direction. The cross product of two vectors can be expressed as in Equation (22)

$$a \times b = a_x b_y - a_y b_x = \|a\| \|b\| \sin(\omega), \quad (22)$$

where ω is an angle from a to b .

The curvature, $\kappa(t)$ of a parametric curve, $m(t)$ and its derivative, $m'(t)$ is defined as follows:

$$\kappa(t) = \frac{m'(t) \times m''(t)}{\|m'(t)\|^3} = \frac{1}{r}, \quad (23)$$

where r is a radius of curvature and the curvature derivative, $\kappa'(t)$ is given in Equation (24) below

$$\kappa'(t) = \frac{\|m'(t)\|^2 \left(\frac{d}{dt}\right)(m'(t) \times m''(t)) - 3(m'(t) \times m''(t))(m'(t) \cdot m''(t))}{\|m'(t)\|^5}. \quad (24)$$

The absolute error of curvature will be calculated using Equation (25) below:

$$\text{Absolute Curvature Error} = |\text{Approximated Curvature Value} - \text{Exact Curvature Value}|. \quad (25)$$

2.5 C-Shape Transition Curve

One of the important aspect of transition curve as mentioned in [12], in which the curve should satisfy curvature continuity condition in order to fulfill geometric conditions, where

$$\kappa(0) = -\frac{1}{r_0}, \quad \kappa(1) = -\frac{1}{r_1}. \quad (26)$$

Figure 2 shows C-shaped transition curve where four control points and two circles with the same radius are used. The first and second circle contains $C_0 = (x_0, y_0)$, $C_1 = (x_1, y_1)$ with radius, r_0 , r_1 and turning angle, α and β respectively. The distance

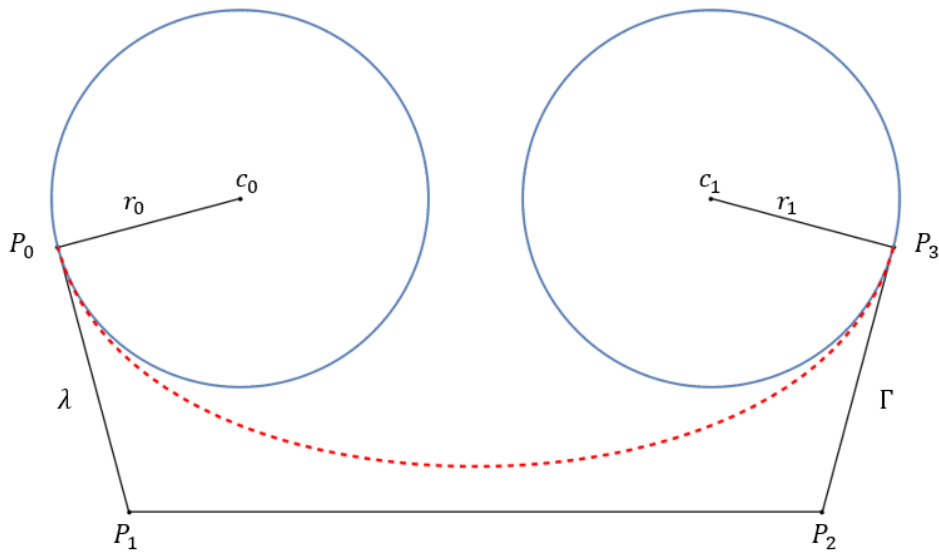


Figure 2. C-shaped transition curve

between the first and second control point is denoted as λ , and the distance between the third and final control point is represented as Γ . The control point P_1 is given as follows:

$$\begin{aligned} P_0 &= C_0 + r_0(\cos(\alpha), -\sin(\alpha)), \\ P_1 &= P_0 - \lambda(\sin(\alpha), \cos(\alpha)), \\ P_2 &= P_3 - \Gamma(-\sin(\beta), \cos(\beta)), \\ P_3 &= C_1 - r_1(\cos(\beta), \sin(\beta)), \end{aligned} \tag{27}$$

where the distance was obtained by solving Equation (26):

$$\lambda = \frac{(-x_0\cos(\beta) + x_1\cos(\beta) + y_0\sin(\beta) - y_1\sin(\beta) + r_0\sin(\alpha + \beta))}{2(\sqrt{\frac{r_1}{r_0}}) + 2(\sqrt{\frac{r_1}{r_0}})\sigma - \cos(\alpha + \beta)}; \tag{28}$$

$$\Gamma = \frac{\sqrt{\frac{r_1}{r_0}}(-x_0\cos(\beta) + x_1\cos(\beta) + y_0\sin(\beta) - y_1\sin(\beta) + r_0\sin(\alpha + \beta))}{2(\sqrt{\frac{r_1}{r_0}}) + 2(\sqrt{\frac{r_1}{r_0}})\sigma - \cos(\alpha + \beta)}. \tag{29}$$

2.6 Travel Time Computation

The travel time without the gravitational force, $T_m(t)$ of the curve is defined as:

$$T_m(t) = \frac{S(t)}{v(t)}, \quad t \in [0, 1], \tag{30}$$

where $S(t)$ is the arc length of the curve, denoted as:

$$S(t) = \int_0^t |b'(t)| dt, \quad t \in [0, 1]. \tag{31}$$

Velocity, $v(t)$ is defined as:

$$v(t) = \int_0^t \sqrt{((x'(t))^2 + (y'(t))^2)}, \quad t \in [0, 1]. \tag{32}$$

Thus, $T_m(t)$ can be expressed as:

$$T_m(t) = \int_0^t \frac{|b'(t)|}{\sqrt{((x'(t))^2 + (y'(t))^2)} dt, \quad t \in [0, 1]. \tag{33}$$

By referring to Equation (6), the travel time under the influence of the gravitational force, $T_g(t)$ is denoted as

$$T_g(t) = \int_0^t \frac{|b'(t)|}{v_g(t)} dt, \quad t \in [0, 1], \tag{34}$$

where $v_g(t) = \sqrt{2gy(t)}$ is the velocity of the curve under the influence of the gravitational force.

2.7 Curve Approximation via C-Shape Transition Curve

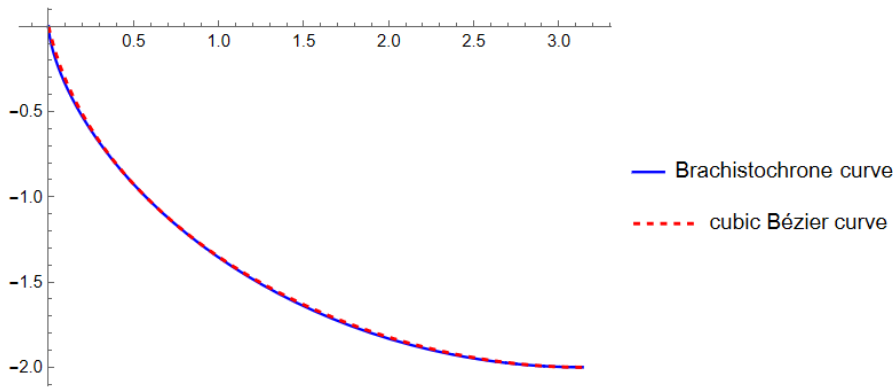


Figure 3. Approximation of Brachistochrone curves using cubic Bézier curve

Figure 3 shows the approximation of Brachistochrone curve using cubic Bézier curve with the same starting point $A(0, 0)$ and ending point $B(3.14, -2)$. Figure 4 shows the approximation of Brachistochrone curve using cubic trigonometric Bézier curve with the same pairs value of the shape parameters ρ and σ while Figure 5 using different pair values of shape parameters. There are three different pairs of shape parameters where $\rho = -2, \sigma = 0$ represented by black dashed curve, $\rho = 0, \sigma = 1$ represented by red dotted curve, and $\rho = 0.5, \sigma = 0$ represented by blue dotted-dashed curve. The black dashed curve and the red dotted curve were obtained close to the Brachistochrone curve.

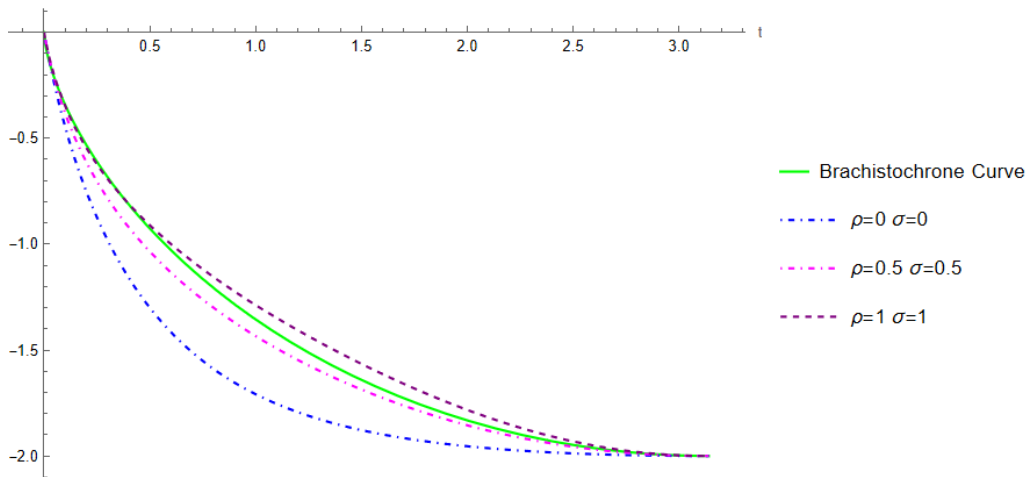


Figure 4. Approximation of Brachistochrone curves using cubic trigonometric Bézier curve with the same pair of shape parameters

The curve was obtained far from the Brachistochrone curve when shape parameters used $\rho = 0.5, \sigma = 0$. Thus, the shape parameters ρ and σ contributed significantly in modifying the curve’s segment while maintaining the control points. Figure 6 shows the closed approximation of Brachistochrone curve using cubic trigonometric Bézier curve with shape parameters $\rho = 0, \sigma = 0.6$. The curve obtained is almost the same as the Brachistochrone when radius of a circle with the turning angle $\alpha = 170$ degree and $\beta = 90$ degree is applied.

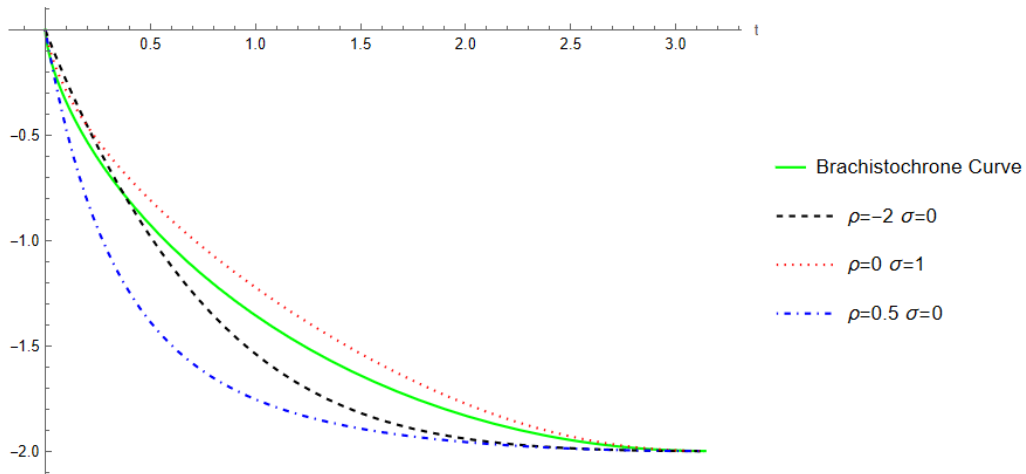


Figure 5. Approximation of Brachistochrone curves using cubic trigonometric Bézier curve with different pairs of shape parameters

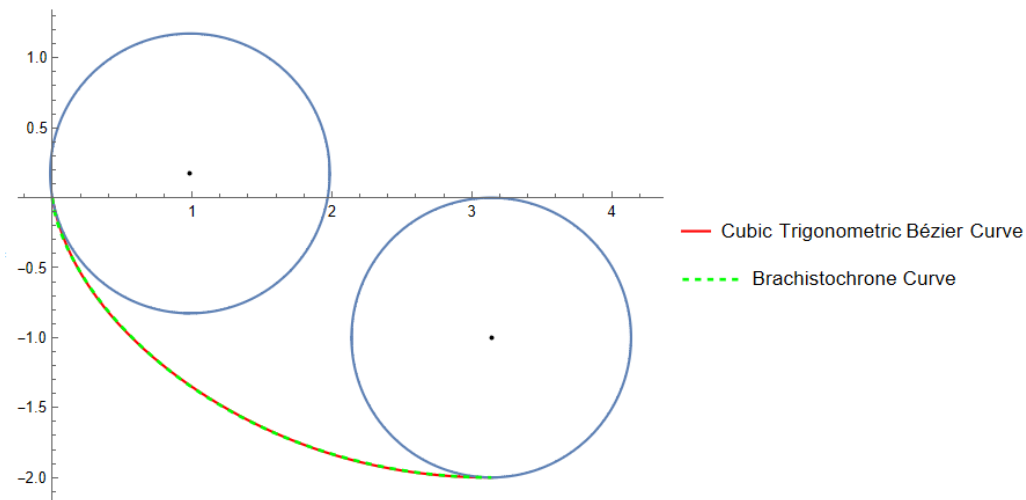


Figure 6. Approximation of Brachistochrone curves using cubic trigonometric Bézier curve with shape parameters $\rho=0, \sigma=0.6$.

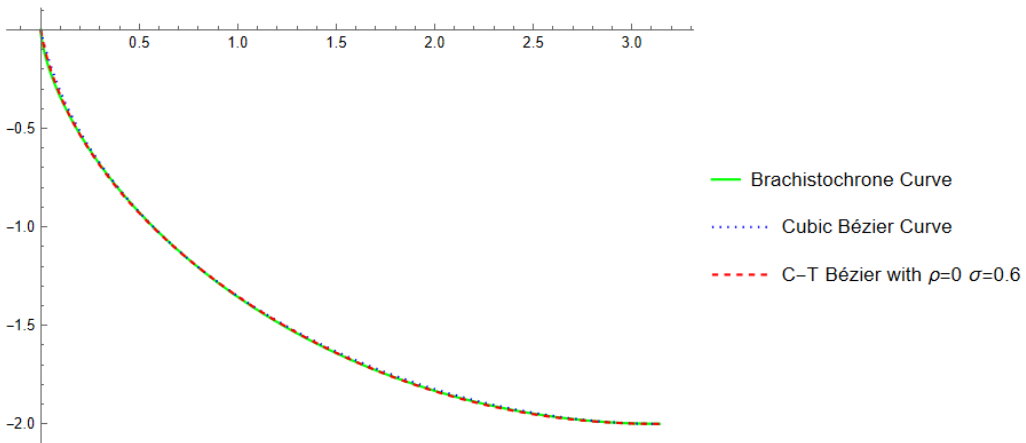


Figure 7. Brachistochrone curve, cubic Bézier curve and cubic trigonometric Bézier curve with shape parameter $\rho=0, \sigma=0.6$

2.8 Travel Time Comparison for Each Curve

Figure 7 displays both approximations of Brachistochrone curve that was obtained using cubic Bézier and cubic trigonometric Bézier curve, while Table 1 shows the comparison between distance, velocity, and travel time with and without the influence of

Table 1. Comparison between distance, velocity, and travel time for each curve

Type of curve	S, m	$v, m/s^{-1}$	$v_g, m/s^{-1}$	T_m, s	T_g, s
Brachistochrone curve	3.99841	2.00000	6.26099	1.99921	1.00329
Cubic Bézier curve	3.99065	3.99000	6.26099	1.00016	1.00463
Cubic trigonometric Bézier curve	3.99766	4.51523	6.26099	0.88537	1.00400

gravitational force. From Table 1, we found that the distance of the cubic Bézier curve and cubic trigonometric Bézier curve only had a slight difference with the Brachistochrone curve, which are 0.00776m and 0.00075m. The same speed was obtained for all curves under the influence of gravitational force.

Travel time without the influence of gravitational force showed that the cubic trigonometric Bézier curve took the shortest travel time of 0.88537s, while cubic Bézier curve takes 1.00016s, and Brachistochrone curve takes 1.99921s. Meanwhile, the travel time under the influence of gravitational force showed that the cubic Bézier curve takes 1.00463s and the cubic trigonometric Bézier curve takes 1.004s to travel along the curve. As a result, the cubic trigonometric Bézier curve provides the closest approximation of Brachistochrone curve when the travel time is under the influence of gravitational force.

3 Curvature Analysis

Figure 8 shows the curvature profiles and Table 2 shows curvature values, velocities, and absolute error for each curve. The actual and the approximated curves shows significant difference in terms of curvature values especially at $t = 0.01$ because Brachistochrone has the same form as an inverted cycloid curve. Cycloid curve is smoother compared to Bézier (or trigonometric Bézier) curve because the cycloid curve is generated by a point on a circle as it rolls along a straight line, while reconstructed curve of Brachistochrone via transition curve using Bézier (or trigonometric Bézier) curve is constructed in different way. This can be validated by observing the curvature profile in Figure 8.

The value of t starts at 0.01 because when $t = 0$, the curvature value is undefined as it shows no movement and speed at the starting point. The increment of 0.1 was then applied to consistently analyse the curvature value and velocity. As the value of t increased, the curvature value decreased because the curve becomes less curvy, thus the speed along the curve increased. The average of absolute curvature values for both Bézier and trigonometric Bézier curves shows a slight different as demonstrated in Table 2. Trigonometric Bézier curve produce lower curvature value on average thus produce higher average of absolute curvature error when comparing with original Brachistochrone curve. Lower curvature value indicates faster speed and shorter travel time. This is supported by the previous discussion in Table 1. Thus, trigonometric Bézier curve produce the closest approximation of Brachistochrone curve in terms of travel time.

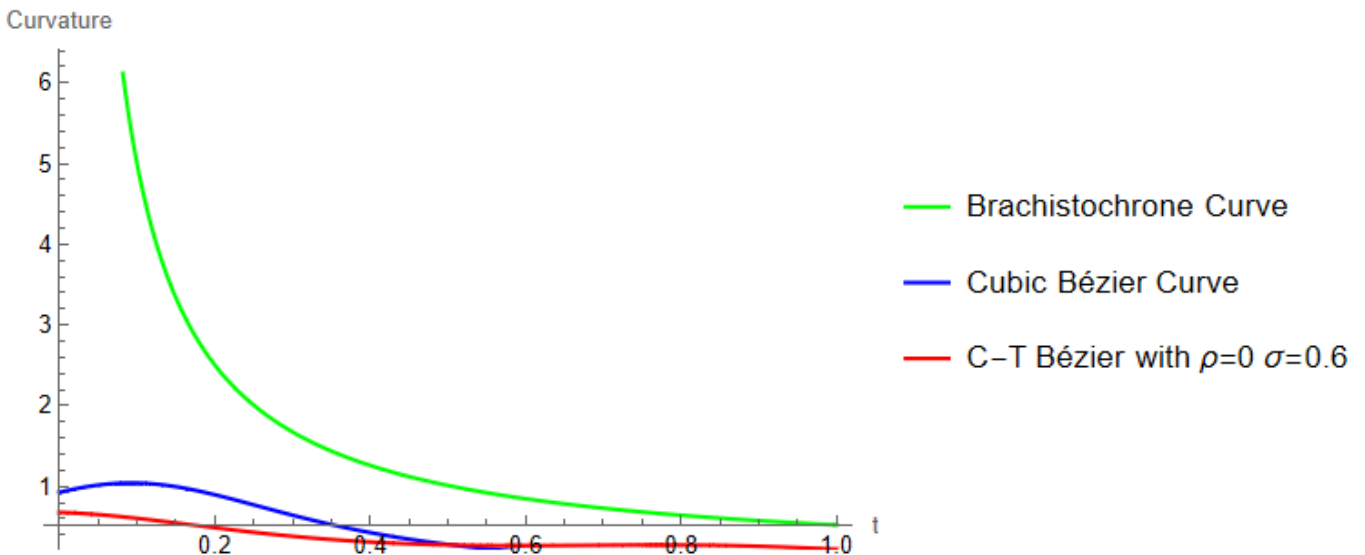


Figure 8. Curvature profile for Brachistochrone curve, cubic Bézier curve, and cubic trigonometric Bézier curve with shape parameter $\rho=0, \sigma=0.6$ via C-shape transition curve

Table 2. Curvature value and velocity for Brachistochrone curve, cubic Bézier curve, and cubic trigonometric Bézier curve with shape parameter $\rho=0, \sigma=0.6$ via C-shape transition curve.

t	Brachistochrone Curve		Cubic Bézier Curve			Cubic Trigonometric Bézier Curve		
	Curvature, κ	Velocity, m/s^{-1}	Curvature, κ	Velocity, m/s^{-1}	Absolute Error	Curvature, κ	Velocity, m/s^{-1}	Absolute Error
0.01	50.000208	0.031305	0.923827	3.76790	49.076381	0.673801	3.47930	49.326407
0.11	4.5477470	0.344181	1.036957	3.73282	3.510790	0.592739	3.59223	3.955008
0.21	2.3853330	0.656197	0.872331	3.78480	1.513002	0.475076	3.76503	1.910257
0.31	1.6193790	0.966572	0.617986	3.88240	1.001393	0.372618	3.93460	1.246761
0.41	1.2280960	1.274530	0.409039	3.99152	0.819057	0.305099	4.05178	0.922997
0.51	0.9910980	1.579310	0.267773	4.08716	0.723325	0.271947	4.10093	0.719151
0.61	0.8325200	1.880130	0.175959	4.15247	0.656561	0.265142	4.10171	0.567378
0.71	0.7192370	2.176260	0.114302	4.17707	0.604935	0.271529	4.09961	0.447708
0.81	0.6344880	2.466950	0.069463	4.15577	0.565025	0.272909	4.14937	0.361579
0.91	0.5688770	2.751470	0.032472	4.08787	0.536405	0.254264	4.29419	0.314613
Average					5.900687			

4 CONCLUSION

Brachistochrone curves are able to be reconstructed using Bézier curve and trigonometric Bézier curve. The presence of shape parameters help in obtaining the close approximation of Brachistochrone curve. Shape parameters provide good adjustability in constructing our target curve. Moreover, the parametric representation of Brachistochrone curve via C-shape transition curve can be used to calculate the distance, velocity, and travel time with and without the influence of gravitational force for each curve. Furthermore, a small change in distance will affect travel time because every curve with the same height has the same speed under the influence of gravitational force. Finally, curvature value can be used to analyse the speed along the curve. The small alteration of shape parameters will change the distance, travel time, curvature value, and speed along the curve.

5 Acknowledgement

This research was supported by Universiti Sains Malaysia under Short Term Grant (STG-Khas) (304/PMATHS/6315587) and School of Mathematical Sciences, Universiti Sains Malaysia. The authors are very grateful to anonymous referees for their valuable suggestion.

REFERENCES

- [1] N. Velasco, D. Vinueza, J. Mármol, D. Mendoza, and F. Pérez. "Experimental demonstration of the Brachistochrone property of the cycloid." In *Journal of Physics: Conference Series* (IOP Publishing, 2019) p. 012075.
- [2] P. C. Deshmukh, P. Rajauria, A. Rajans, B. R. Vyshakh, and S. Dutta. "The brachistochrone." *Resonance* 22, no. 9 (2017): 847-866.
- [3] M. Y. Misro, A. Ramli, and J. M. Ali. "Approximating maximum speed on road from curvature information of Bézier curve." *World Academy of Science, Engineering and Technology, International Journal of Mathematical, Computational, Physical, Electrical and Computer Engineering* 9, 705-712 (2015)
- [4] M. F. Ibrahim, M. Y. Misro, A. Ramli, and J. M. Ali. "Maximum safe speed estimation using planar quintic Bézier curve with C2 continuity." In *AIP Conference Proceedings* (AIP Publishing LLC, 2017) p.050006
- [5] M. Y. Misro, A. Ramli, and J. M. Ali. "Quintic trigonometric Bézier curve and its maximum speed estimation on highway designs." In *textitAIP conference proceedings* (AIP Publishing LLC, 2018) p. 020089
- [6] X. A. Han, Y. Ma, and X. Huang. "The cubic trigonometric Bézier curve with two shape parameters." *Applied Mathematics Letters* 22, no. 2 (2009): 226-231.
- [7] S. BiBi, M. Y. Misro, M. Abbas, A. Majeed, and T. Nazir. "G3 Shape Adjustable GHT-Bézier Developable Surfaces and Their Applications." *Mathematics* 9(19) (2021) p.2350.
- [8] S. A. A. S. M. Zain, M. Y. Misro, and K. T. Miura. "Generalized fractional Bézier curve with shape parameters." *Mathematics* 9(17) (2021) p. 2141.

- [9] M. Ammad, M. Y. Misro, and A. Ramli. "A novel generalized trigonometric Bézier curve: Properties, continuity conditions and applications to the curve modeling." *Mathematics and Computers in Simulation* 194 (2022): 744-763.
- [10] D. S. Meek, and D. J. Walton. "Spiral arc spline approximation to a planar spiral." *Journal of Computational and Applied Mathematics* 107(1) (1999): 21-30.
- [11] Z. Habib, and M. Sakai. "G 2 planar cubic transition between two circles." *International Journal of Computer Mathematics* 80(8) (2003): 957-965.
- [12] M. Y. Misro, A. Ramli, and J. M. Ali. "S-shaped and c-shaped transition curve using cubic trigonometric Bézier." In *AIP Conference Proceedings* (AIP Publishing LLC, 2017) p. 050005.
- [13] M. Y. Misro, A. Ramli, and J. M. Ali. "Extended analysis of dynamic parameters on cubic trigonometric Bézier transition curves." In *2019 23rd International Conference in Information Visualization–Part II*(IEEE, 2019) pp. 141-146
- [14] M. Y. Misro, A. Ramli, J. M. Ali, and N. N. A. Hamid. "Pythagorean hodograph quintic trigonometric Bézier transtion curve." In *2017 14th International Conference on Computer Graphics, Imaging and Visualization*(IEEE, 2017) pp. 1-7.
- [15] S. BiBi, M.Y. Misro, and M. Abbas. "Smooth path planning via cubic GHT-Bézier spiral curves based on shortest distance, bending energy and curvature variation energy." *AIMS Mathematics* 6(8) (2021): 8625-8641.
- [16] Y. Nishiyama, "The brachistochrone curve: The problem of quickest descent." *International Journal of Pure and Applied Mathematics* 82(3) (2013), 409-419.
- [17] S. Gómez-Aíza, R. W. Gómez, and V. Marquina. "A simplified approach to the brachistochrone problem." *European Journal of physics* 27, no. 5 (2006): 1091.
- [18] R. Padyala, "Brachistochrone–the path of quickest descent." *Resonance* 24, no. 2 (2019): 201-216.
- [19] Z. Habib, and M.Sakai. "G2 cubic transition between two circles with shape control." *Journal of Computational and Applied Mathematics* 223 (1) (2009): 133-144.